Developing and Evaluating a Nomogram Model Predicting Axillary Lymph Node Metastasis of Triple-Negative Breast Cancer Based on Multimodal Imaging Characteristics

Yantong Jin,[1] Xingyuan Liu,[1] Xingda Zhang, Yang Wang, Xiaoying Cheng, Siwei Cao, Wuyue Zhang, Mingming Zhao, Ye Ruan, Bo Gao

Rationale and Objectives: Breast cancer is the most frequently diagnosed cancer among women worldwide, with axillary lymph nodes being common sites of metastasis, particularly triple-negative breast cancer (TNBC), which is the subtype with the poorest prognosis. This study aimed to develop a nomogram model to predict axillary lymph node metastasis (ALNM) in TNBC patients based on mammography (MG), multimodal ultrasound (US), and clinical pathological characteristics.

Patients and Methods: A retrospective study was performed on 291 patients diagnosed with TNBC from two centers. Patients from the Center 1 were randomly divided into a training cohort (n = 159) and a internal test cohort (n = 68) using a 7:3 ratio, while patients from the Center 2 served as an external test cohort. Each group was further divided into an ALNM group and a non-ALNM group based on the presence or absence of ALNM. Predictors were selected via least absolute shrinkage and selection operator (LASSO) regression and multivariable logistic analysis. The predictive performance of the nomogram model was evaluated by the receiver operating characteristic curve (ROC), calibration curve, and decision curve analysis (DCA).

Results: Notable predictors included MG_reported_margin, MG_reported_suspicious malignant calcifications, MG_reported_abnormal ALN, elastography score, and US_reported_abnormal ALN. The area under the receiver operating characteristics curve (AUC) value of the nomogram model was 0.931 (95%CI: 0.890–0.973) for the training cohort, AUC=0.929 (95%CI: 0.871–0.986) for the internal test cohort and AUC=0.891 (95%CI: 0.794–0.987) for the external test cohort. Calibration curves and DCA both suggested that the nomogram exhibited favorable calibration and clinical utility.

Conclusion: The predictive model combined with multimodal US and MG characteristics developed in this study is highly accurate, serves as a powerful tool for clinical assessment, and shows promise for predicting ALNM in patients with TNBC.

Key Words: Triple-negative breast cancer; Mammography; Multimodal ultrasound; Axillary lymph node metastasis; Nomogram.

Abbreviation: BC breast cancer, **TNBC** triple-negative breast cancer, **ALN** axillary lymph node, **ALNM** axillary lymph node metastasis, **AUC** area under the curve, **DBT** digital breast tomosynthesis, **DCA** decision curve analysis, **DCE-MRI** dynamic contrast-enhanced magnetic resonance imaging, **ER** estrogen receptor, **HER-2** human epidermal growth factor receptor-2, **LASSO** Least Absolute Shrinkage and Selection Operator, **MG** mammography, **MRI** magnetic resonance imaging, **NLR** neutrophil to lymphocyte ratio, **PR** progesterone receptor, **ROC** receive operating characteristic, **US** ultrasound

Acad Radiol 2025; 32:4382–4394

From the Department of Radiology, The Second Affiliated Hospital of Harbin Medical University, Harbin 150086, China (Y.J., X.L., Y.W., X.C., S.C., M.Z., Y.R., B.G.); Department of Breast Surgery, Harbin Medical University Cancer Hospital, Harbin 150081, China (X.Z.); Department of Ultrasound, The Second Affiliated Hospital of Harbin Medical University, Harbin 150086, China (W.Z.). Received January 7, 2025; revised March 27, 2025; accepted April 11, 2025. **Address correspondence to**: B.G. e-mail: gaobo72519@hrbmu.edu.cn

[1] Yantong Jin and Xingyuan Liu contributed equally to this work.

https://doi.org/10.1016/j.acra.2025.04.031

INTRODUCTION

Breast cancer (BC) emerges as the leading type of cancer affecting women globally (1). Among the various metastatic sites of BC, axillary lymph node metastasis (ALNM) is a common occurrence that significantly affects clinical staging, treatment, and prognosis, and is also an indication for neoadjuvant chemotherapy (2,3). A Study indicates the 5-year survival rate for BC patients without ALNM can climb up to 99.0%, whereas those with ALNM tend to decrease to 86.0% (1). When it comes to treating triple-negative breast cancer (TNBC), clinicians face unique challenges due to the nature of this particular subtype (4,5). Studies have demonstrated that TNBC patients are at a greater risk of developing ALNM, making it crucial to predict lymph node status before surgery accurately (3). This information is essential for determining individualized treatment plans and assessing the prognosis of TNBC patients.

Sentinel lymph node biopsy and axillary lymph node dissection are the standard methods for evaluating axillary lymph node (ALN) status in BC patients (6). However, they are both invasive procedures that can lead to complications such as lymphedema, paresthesia and restricted arm movement (7,8). Sentinel lymph node biopsy still has a specific rate of false negative results (9). Fine-needle aspiration biopsy (FNAB) uses a thin needle to obtain tissue samples, providing rapid and minimally invasive pathological results (10). However, it is technically demanding to perform on deep lymph nodes and may result in false-negative outcomes (11). Many imaging examinations can assess the status of ALN non-invasively and flexibly, but conventional methods primarily rely on morphological changes in ALN, which have certain limitations. Ultrasound (US) is an essential method for assessing ALNM in BC. Still, there is some overlap in the US characteristics of metastatic lymph nodes and benign reactive lymph nodes, resulting in a particular proportion of false positive rates (12). Moreover, it is influenced by subjective experience (12). While mammography (MG) is advantageous in detecting microcalcifications, it may fail to display some axillary areas due to factors like projection techniques and image field limitations, which can reduce its sensitivity in identifying ALNM (3). Finally, magnetic resonance imaging (MRI) has high sensitivity in identifying lymph nodes, but its specificity is limited (13). Therefore, clinicians urgently need a non-invasive, accurate and simple method to predict the ALN status of TNBC patients early.

The imaging characteristics of primary lesions in BC are associated with tumors' biological behavior, which could contribute to predicting the status of ALN (3,14). While some studies have explored the relationship between imaging characteristics of TNBC (such as breast MG, US, and MRI) and ALNM, most have only used one imaging technique and produced inconsistent results (5,15,16).

In the present study, we aimed to develop a new nomogram based on multimodal imaging characteristics for ALNM prediction in TNBC patients. This would enable surgeons to avoid unnecessary procedures with a noninvasive and cost-effective approach.

MATERIAL AND METHODS

Database

Our study was conducted according to the ethical standards of the 2013 revised Declaration of Helsinki for studies involving human participants. Our medical ethics committee approved the retrospective study. The patients who participated in our study provided their written informed consent.

From January 2013 to June 2023 and from January to December 2024, a retrospective study was conducted in Centers 1 and 2, including 282 and 78 female patients, respectively, with histopathological confirmed TNBC. The inclusion criteria were as follows: 1. MG and multimodal US examinations were performed within one week before surgery at our hospital, and complete clinical and pathological data were available; 2. Unilateral solitary lesion; 3. No acute or chronic inflammation and hematologic disorders before surgery. The exclusion criteria were as follows: 1. Needle puncture or histological biopsy of mass or ALN before the multimodal US; 2. Treated with neoadjuvant chemotherapy or radiotherapy before surgery; 3. Non-mass lesions; 4. Patients with stage IV at the initial diagnosis. A total of 291 TNBC patients from Center 1 and Center 2 were finally included in the study (Fig 1). The enrolled patients from Center 1 were randomly divided into training and test cohorts at a 7:3 ratio. Each cohort was further categorized into ALNM and non-ALNM groups based on pathological examination results. The enrolled patients from Center 2 were used as an external validation cohort.

Image Acquisitions and Analysis

MG examination was performed using Hologic Selenia full digital MG camera (Hologic Medical Systems, Boston, MA), with routine imaging of both breasts in the craniocaudal and mediolateral oblique views. Two radiologists with 10 and 15 years of experience in MG diagnosis from each center blindly evaluated the MG images according to the American College of Radiology and BI-RADS 5th edition standard. If the opinions of the radiologists differed, another radiologist with more than 15 years of experience reviewed the case and resolved the disagreement.

The recorded characteristics included: quadrant, MG_reported_ glandular density, MG_reported_maximum diameter, MG_reported_mass density, MG_reported_shape, MG_reported_margin, MG_reported_suspicious malignant calcifications, MG_reported_abnormal ALN and MG_reported_skin thickening or induration (Table 1). MG_reported_suspicious malignant calcifications within the mass were presenting as: 1. amorphous; 2. coarse heterogeneous; 3. fine pleomorphic; 4. fine linear; 5. fine-linear branching distribution. The presence of one or more of these

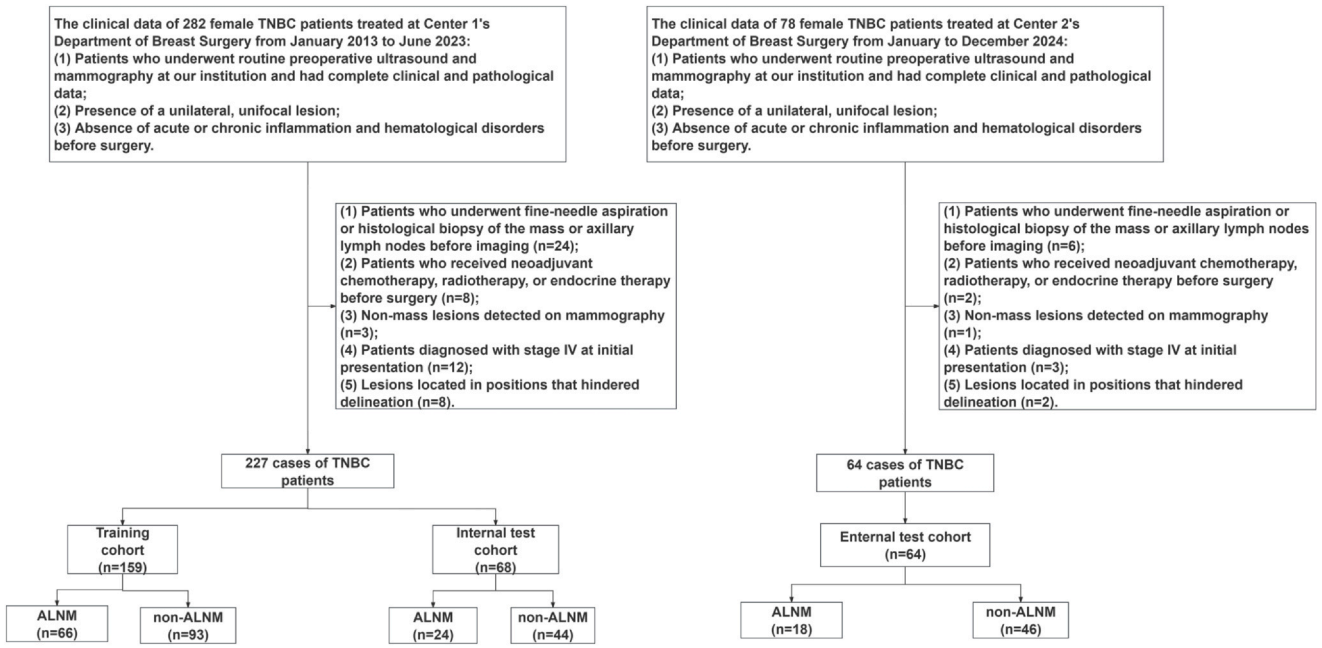

Figure 1. Flowchart of the enrollment process. ALNM, axillary lymph node metastasis; TNBC, triple-negative breast cancer.

characteristics indicated MG_reported suspicious malignant calcifications. In addition, the criteria for diagnosing MG_reported_abnormal ALN were as follows: 1. lymph node enlargement with a round shape and a short-axis diameter of ≥10 mm (3); 2. cortical thickening of the lymph node; 3. disappearance of the fatty hilum; 4. unclear margins or speculation, presence of suspicious malignant calcifications (17). The presence of one or more of these characteristics was considered indicative of MG_reported_abnormal ALN.

Breast multimodal US examinations were performed using the Acuson S2000 system (Siemens Medical Solutions, Mountain View, CA) with a 5–12 MHz linear array transducer at Center 1 and the Acuson Sequoia ultrasound system with a 10L4 linear array probe (frequency: 10 MHz) at

TABLE 1. Patient Demographics and Baseline Characteristics

Characteristic	Cohort				*P-value*
	Overall (n = 291)	Training Cohort (n = 159)	Internal Test Cohort (n = 68)	External Test Cohort (n = 64)	
Age					0.901
M (Q1, Q3)	52 (45, 61)	52 (45, 61)	52 (47, 57)	55 (44, 61)	
NLR					0.823
M (Q1, Q3)	1.94 (1.57, 2.44)	1.93 (1.50, 2.38)	1.95 (1.65, 2.40)	1.90 (1.54, 2.52)	
Menstrual status					0.934
Unfinished	126 (43.3%)	68 (42.8%)	29 (42.6%)	29 (45.3%)	
Finished	165 (56.7%)	91 (57.2%)	39 (57.4)	35 (54.7%)	
KI–67					0.048
M (Q1, Q3)	70 (40, 80)	70 (40, 80)	70 (50, 80)	60 (39, 71)	
Tumor histologic grade					0.009
Grade I or II	60 (20.6%)	26 (16.4%)	12 (17.6%)	22 (34.4%)	
Grade III	231 (79.4%)	133 (83.6%)	56 (82.4%)	42 (65.6%)	
Tumor histologic type					0.023
Invasive ductal carcinoma	270 (92.8%)	151 (95.0%)	65 (95.6%)	54 (84.4%)	
Others	21 (7.2%)	8 (5.0%)	3 (4.4%)	10 (15.6%)	
MG_reported_maximum diameter					0.621
M (Q1, Q3)	2.30 (1.80, 3.10)	2.30 (1.80, 3.00)	2.35 (1.90, 3.03)	2.25 (1.50, 3.20)	
Quadrant					0.871
Others	122 (41.9%)	68 (42.8%)	29 (42.6%)	25 (39.1%)	
Upper outer quadrant	169 (58.1%)	91 (57.2%)	39 (57.4%)	39 (60.9%)	

Table 1 (*Continued*)

Characteristic	Cohort				*P-value*
	Overall (n = 291)	Training Cohort (n = 159)	Internal Test Cohort (n = 68)	External Test Cohort (n = 64)	
MG_reported_glandular density					0.364
Non-dense (Fatty, Scattered fibroglandular)	150 (51.5%)	86 (54.1%)	36 (52.9%)	28 (43.8%)	
Dense (Heterogeneously dense, Extremely dense)	141 (48.5%)	73 (45.9%)	32 (47.1%)	36 (56.3%)	
MG_reported_mass density					0.060
Iso-density	155 (53.3%)	94 (59.1%)	34 (50.0%)	27 (42.2%)	
High density	136 (46.7%)	65 (40.9%)	34 (50.0%)	37 (57.8%)	
MG_reported_shape					0.600
Round, oval	115 (39.5%)	59 (37.1%)	30 (44.1%)	26 (40.6%)	
Irregular	176 (60.5%)	100 (62.9%)	38 (55.9%)	38 (59.4%)	
MG_reported_margin					0.767
Non-spiculated	204 (70.1%)	109 (68.6%)	48 (70.6%)	47 (73.4%)	
Spiculated	87 (29.9%)	50 (31.4%)	20 (29.4%)	17 (26.6%)	
MG_reported_suspicious malignant calcifications					0.851
Negative	188 (64.6%)	105 (66.0%)	43 (63.2%)	40 (62.5%)	
Positive	103 (35.4%)	54 (34.0%)	25 (36.8%)	24 (37.5%)	
MG_reported_ abnormal ALN					0.601
Absent	213 (73.2%)	114 (71.7%)	49 (72.1%)	50 (78.1%)	
Present	78 (26.8%)	45 (28.3%)	19 (27.9%)	14 (21.9%)	
MG_reported_skin thickening or induration					0.228
Negative	250 (85.9%)	138 (86.8%)	61 (89.7%)	51 (79.7%)	
Positive	41 (14.1%)	21 (13.2%)	7 (10.3%)	13 (20.3%)	
US_resported_echo pattern					0.877
Homogeneous	61 (21.0%)	35 (22.0%)	13 (19.1%)	13 (20.3%)	
Heterogeneous	230 (79.0%)	124 (78.0%)	55 (80.9%)	51 (79.7%)	
US_resported_posterior acoustic decrease					0.217
Negative	246 (84.5%)	139 (87.4%)	57 (83.8%)	50 (78.1%)	
Positive	45 (15.5%)	20 (12.6%)	11 (16.2%)	14 (21.9%)	
US_resported_hyperechoic halo					0.061
Negative	233 (80.1%)	134 (84.3%)	54 (79.4%)	45 (70.3%)	
Positive	58 (19.9%)	25 (15.7%)	14 (20.6%)	19 (29.7%)	
Color Doppler flow					0.153
0-I	43 (14.8%)	22 (13.8%)	7 (10.3%)	14 (21.9%)	
II-III	248 (85.2%)	137 (86.2%)	61 (89.7%)	50 (78.1%)	
Elastography score					0.074
1 or 2 or 3	153 (52.6%)	84 (52.8%)	29 (42.6%)	40 (62.5%)	
4 or 5	138 (47.4%)	75 (47.2%)	39 (57.4%)	24 (37.5%)	
US_resported_ abnormal ALN					0.556
Absent	128 (44.0%)	71 (44.7%)	29 (42.6%)	28 (43.8%)	
Present (with normal blood flow)	93 (32.0%)	45 (28.3%)	24 (35.3%)	24 (37.5%)	
Present (with abnormal blood flow)	70 (24.1%)	43 (27.0%)	15 (22.1%)	12 (18.8%)	

NLR, neutrophil to lymphocyte ratio; MG, mammography; US, ultrasound; ALN, axillary lymph node.

Center 2. The patient was in a supine position with arms elevated and both breasts and axillae fully exposed. At each center, two radiologists, each with over 5 years of experience in breast US diagnosis, collectively analyzed and evaluated the multimodal US images according to the ACR Breast Imaging Reporting and Data System (BI-RADS, 2nd edition) standards, without knowledge of the pathological results. If the opinions of the two radiologists differed, another radiologist with more than 10 years of experience reviewed the case and resolved the disagreement.

The recorded characteristics included: US_reported_ echo pattern, US_reported_posterior acoustic decrease,

US_reported_hyperechoic halo, US_reported_ abnormal ALN, color Doppler flow and elastography score. According to Adler's classification, the CDFI blood flow sonograms were classified into Grade 0-I and Grade II-III (18). The criteria for diagnosing the US_reported_ abnormal ALN were as follows: 1. Focal cortical bulging or unclear corticomedullary differentiation; 2. a longitudinal to a transverse ratio greater than one or a round shape, abnormal volume increase; 3. complete or partial disappearance of the hilum structure; 4. peripheral vascular formation shown by Doppler US (17,19). If one or more of these characteristics were present, it was considered US_reported_ abnormal ALN. The criteria for elastography score were as follows: 1. a score of 1 indicated entire lesion completely green inside; 2. a score of 2 indicated entire lesion primarily green, with a small amount of blue; 3. a score of 3 indicated entire lesion showed green and blue alternately and roughly equal proportions; 4. a score of 4 indicated entire lesion appeared blue (possibly with a small amount of green); 5. a score of 5 indicated entire lesion and surrounding areas all seemed to be blue (possibly with a small amount of green) (20).

Clinicopathological Characteristics Evaluation

All specimens were examined for pathological type and histological grade by hematoxylin and eosin staining. Immunohistochemistry was used to detect the expression of estrogen receptor, progesterone receptor, human epidermal growth factor receptor-2, and Ki-67. Estrogen/progesterone receptor results: negative if less than 1% of tumor cells show nuclear staining, positive if 1% or more. Human epidermal growth factor receptor-2 results: negative for 0 or 1+, positive for 3+, and 2+ requires further confirmation by fluorescence in situ hybridization amplification (21).

Patient age, neutrophil to lymphocyte ratio (NLR), menstrual status, tumor histological grading, Ki-67 proliferation index, and pathological type were retrieved from the electronic medical record systems of Centers 1 and 2. Age, NLR, and Ki-67 proliferation index were recorded as continuous variables. Histological grading was recorded as a categorical variable, divided into a low-grade group (Grade I and Grade II) and a high-grade group (Grade III) (Table 1).

Development and Evaluation of the Nomogram Model

To minimize the effect of multicollinearity among predictors and to avoid model overfitting, this study employed the least absolute shrinkage and selection operator (LASSO) regression and multivariable binary logistic regression for variable selection and model construction. First, the penalty parameter was adjusted using 10-fold cross-test to determine the optimal regularization coefficient (lambda, λ) for the LASSO regression. Then, based on the λ value (lambda.1se) corresponding to the one standard error of the minimum mean squared error, variables with non-zero parameters were selected as predictors for inclusion in the multivariable logistic regression analysis. Finally, a multivariable binary logistic regression analysis was used to identify the final set of predictors for developing the nomogram model.

The performance of the models was evaluated using the receiver operating characteristic (ROC) curves and area under the receiver operating characteristics curve (AUC), specificity, sensitivity, negative predictive value, and positive predictive value. The calibration curve was used to compare the consistency between predicted probability and actual probability, while decision curve analysis (DCA) was employed to evaluate the effectiveness of different clinical decision strategies.

Statistical Analysis

All analyses were conducted using R software (version 4.2.2) for statistical analysis using two-sided tests, with $p < 0.05$ indicating statistical significance. The normality test of the continuous variables was assessed using the Shapiro-Wilk normality test. The continuous variables that do not follow a normal distribution are represented by M (Q1, Q3), and non-parametric tests tested their association with ALNM. The categorical variables were represented by the relative frequencies (%), and their association with ALNM was tested by the $\chi 2$ test or Fisher's exact test.

RESULTS

Clinicopathological and Imaging Characteristics

291 patients with TNBC were finally enrolled and were assigned to the training cohort (n=159), internal test cohort (n=68), and external test cohort (n=64). Of the 227 patients enrolled at Center 1, 90 patients (39.6%) had ALNM, while 137 patients (60.4%) did not have ALNM. Of the 64 patients enrolled at Center 2, 18 patients (28.1%) had ALNM, while 46 patients (71.9%) did not have ALNM. Baseline characteristics were presented in Table 1. Table 1 showed no significant differences in the characteristics among the three cohorts, indicating good consistency, except for a few clinical characteristics. In the training cohorts, MG_reported_suspicious malignant calcifications, MG_reported_margin, MG_reported_abnormal ALN, MG_report_Skin.thickening.or.induration, US_reported_abnormal ALN and elastography score all showed significant differences between the ALNM and non-ALNM groups (Supplemental table 1).

Predictors Selection

In the training cohort, no characteristics were selected in clinicopathological characteristics through LASSO regression analysis. Based on imaging characteristics, 10 predictors were selected, of which 6 originated from MG characteristics (quadrant, MG_reported_maximum diameter, MG_reported_margin, MG_reported_suspicious malignant calcifications, MG_reported_skin thickening or induration and MG_reported_abnormal ALN) and 4 from multimodal US characteristics (US_reported_posterior acoustic decrease,

TABLE 2. The Coefficients of LASSO Regression Analysis

Coefficient	Variable
−2.535656602	(Intercept)
0.009854437	MG_reported_maximum.diameter_level_
0.000000000	Age_level_
0.000000000	NLR_level_
0.328462169	Quadrant_level_1
0.000000000	Color.Doppler.flow_level_1
0.897336153	Elastography.score_level_1
0.016790926	US_resported_posterior.acoustic.decrease_level_1
0.000000000	US_resported_echo.pattern_level_1
0.701101240	US_reported_.abnormal.ALN_level_1
0.771263133	US_reported_.abnormal.ALN_level_2
0.000000000	Ki67_level_
0.061229413	US_resported_hyperechoic.halo_level_1
0.000000000	MG_reported_.glandular.density_level_2
0.000000000	MG_reported_mass.density_level_2
0.000000000	MG_reported_shape_level_2
0.295304419	MG_reported_suspicious malignant calcifications_level_1
1.224711418	MG_reported_margin_level_2
2.051557068	MG_reported_.abnormal.ALN_level_1
0.003304397	MG_reported_skin.thickening.or.induration_level_1
0.000000000	Histological.grade_level_2
0.000000000	Menstrual.status_level_1
0.000000000	Histologic.type_level_2

NLR, neutrophil to lymphocyte ratio; MG, mammography; US, ultrasound; ALN, axillary lymph node.

US_reported_hyperechoic halo, elastography score and US_reported_abnormal ALN) (Table 2, Fig 2). These 10 predictors were included in further multivariate binary logistic regression analysis. The results of the analysis showed that MG_reported_margin, MG_reported_suspicious malignant calcifications and MG_reported_abnormal ALN as independent predictors for ALNM in patients with TNBC. Multimodal US images with elastography score and US_reported_abnormal ALN were also identified as independent predictors for ALNM in TNBC patients (Table 3). Typical case images are shown in Figure 3 and Figure 4.

Establishment and Evaluation of Nomogram

Based on the results of multivariate logistic regression analysis, we constructed a nomogram to predict ALNM in TNBC patients (Fig 5). This model predicted ALNM in TNBC patients in the training cohort with an accuracy of 88.7%, a sensitivity of 83.3%, specificity of 92.5%, positive predictive value of 88.7%, and negative predictive value of 88.7% (Table 4).

The AUCs of the ALN metastasis rate based on the predictors in the training cohort, including MG_reported_margin, MG_reported_suspicious malignant calcifications,

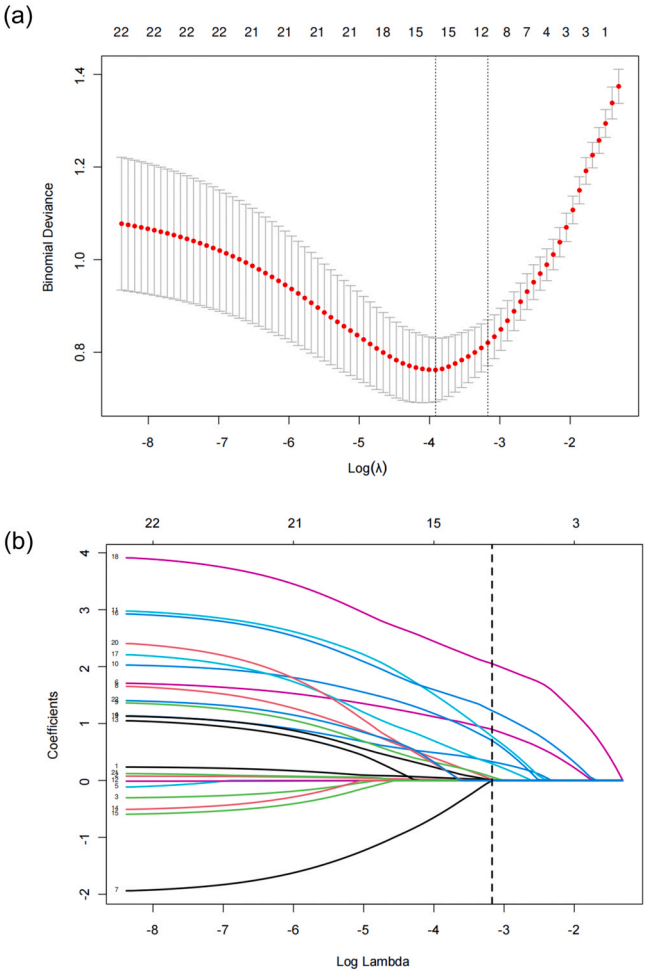

Figure 2. Characteristics selection via LASSO regression model. (**a**) Selecting lambda.1se via10-fold cross-validation. (**b**) LASSO profiles for the 21 baseline characteristics.

MG_reported abnormal ALN, elastography score and US_reported _abnormal ALN were 0.672 (95% CI: 0.600–0.744), 0.624 (95% CI: 0.549–0.699), 0.750 (95% CI: 0.684–0.816), 0.693 (95% CI: 0.619–0.766) and 0.752 (95% CI: 0.680–0.825), respectively (Fig 6a, Supplemental table 2). The nomogram AUC was 0.931 (95% CI: 0.890–0.973) in the training cohort, 0.929 (95% CI: 0.871–0.986) in the internal test cohort, and 0.891 (95%CI: 0.794–0.987) in the external test cohort (Fig 6b, Table 4), outperforming the individual predictors and indicating excellent performance of the nomogram.

The calibration curve showed good consistency between the predicted probability and the actual probability (Fig 7). The DCA indicated the model has good clinical utility in the training and test cohorts (Fig 8).

DISCUSSION

TNBC is a heterogeneous subtype of BC that accounts for 15–20% of all cases and is associated with a poor prognosis

TABLE 3. Results of Multivariate Logistic Regression for Training Cohort

Characteristic	OR	95% CI	*P-value*
MG_reported_margin			
Non-spiculated	—	—	
Spiculated	11.33	3.41, 37.69	< 0.001
MG_reported_suspicious malignant calcifications			
Negative	—	—	
Positive	3.81	1.20, 12.08	0.023
MG_reported_ abnormal ALN			
Absent	—	—	
Present	25.19	6.82, 93.08	< 0.001
US_reported_ abnormal ALN			
Absent	—	—	
Present (with normal blood flow)	9.17	2.68, 31.38	< 0.001
Present (with abnormal blood flow)	10.24	2.58, 40.70	< 0.001
Elastography score			
1 or 2 or 3	—	—	
4 or 5	6.07	2.06, 17.89	0.001

NLR, neutrophil to lymphocyte ratio; MG, mammography; US, ultrasound; ALN, axillary lymph node; OR, odd ratio; CI, confidence interval.

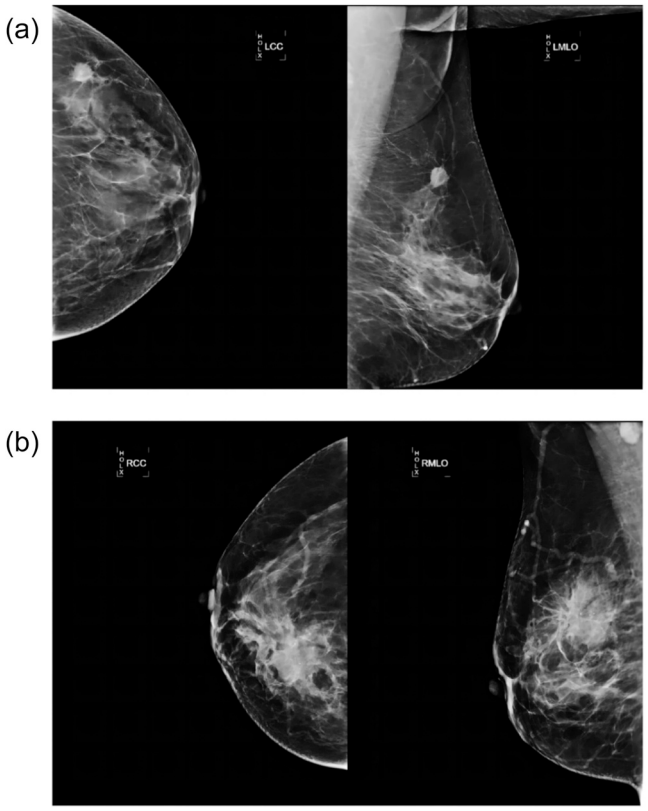

Figure 3. Typical MG characteristics in TNBC patients with non-ALNM present or ALNM present. (**a**) A 58-year-old TNBC patient without ALNM presented with a round, equal dense mass with obscured margins in the left breast, measuring approximately 1.3 cm in maximum diameter. The mass showed no associated microcalcifications, and no suspicious lymph nodes were observed in the LMLO view. (**b**) A 55-year-old TNBC patient with ALNM presented with an irregular-shaped equal dense mass with spiculated margins in the right breast, measuring approximately 3.6 cm in maximum diameter. The mass showed associated microcalcifications, and suspicious lymph nodes were observed in the RMLO view.

(22). Accurate preoperative prediction of ALN status is critical for clinically staging and treating TNBC patients, as ALNM is a significant prognostic factor (23). Nomogram models based on imaging characteristics from breast MG, MRI and US have been constructed to predict an ALNM in BC patients (2,24,25). There is a lack of studies on the prediction model of TNBC imaging characteristics and ALNM, and the conclusions are inconsistent. Our study aimed to explore the predictors of ALNM in TNBC patients. Specifically, we constructed a nomogram model by combining MG imaging characteristics with multimodal US imaging characteristics and clinicopathological characteristics. This model is intended to provide valuable references for the preoperative prediction of ALNM in TNBC patients.

The current BC ALNM prediction model had limited predictive ability for the TNBC population. Wang et al used a logistic regression model based on US characteristics to predict ALNM in TNBC patients, with an AUC value of 0.6898 (16). Song et al analyzed MRI characteristics and used three machine learning algorithms (support vector machine, random forest, logistic regression) to evaluate lymph node metastasis in TNBC patients, with the maximum AUC value obtained by the three algorithms being 0.74 (15). Due to the relatively low proportion of TNBC patients, there has been limited study on the related predictors of ALNM, and there is some disagreement on the predictors. Moreover, the general BC ALNM prediction models have very limited predictive ability for the TNBC population. In addition to this, an external validation was incorporated to further assess the robustness and generalization capabilities of the developed model. Ultimately, the prediction model we established demonstrated an AUC of 0.931, an accuracy of 88.7%, a sensitivity of 83.3%, a specificity of 92.5%, a positive predictive value of 88.7%, and a negative predictive value of 88.7%; within the internal

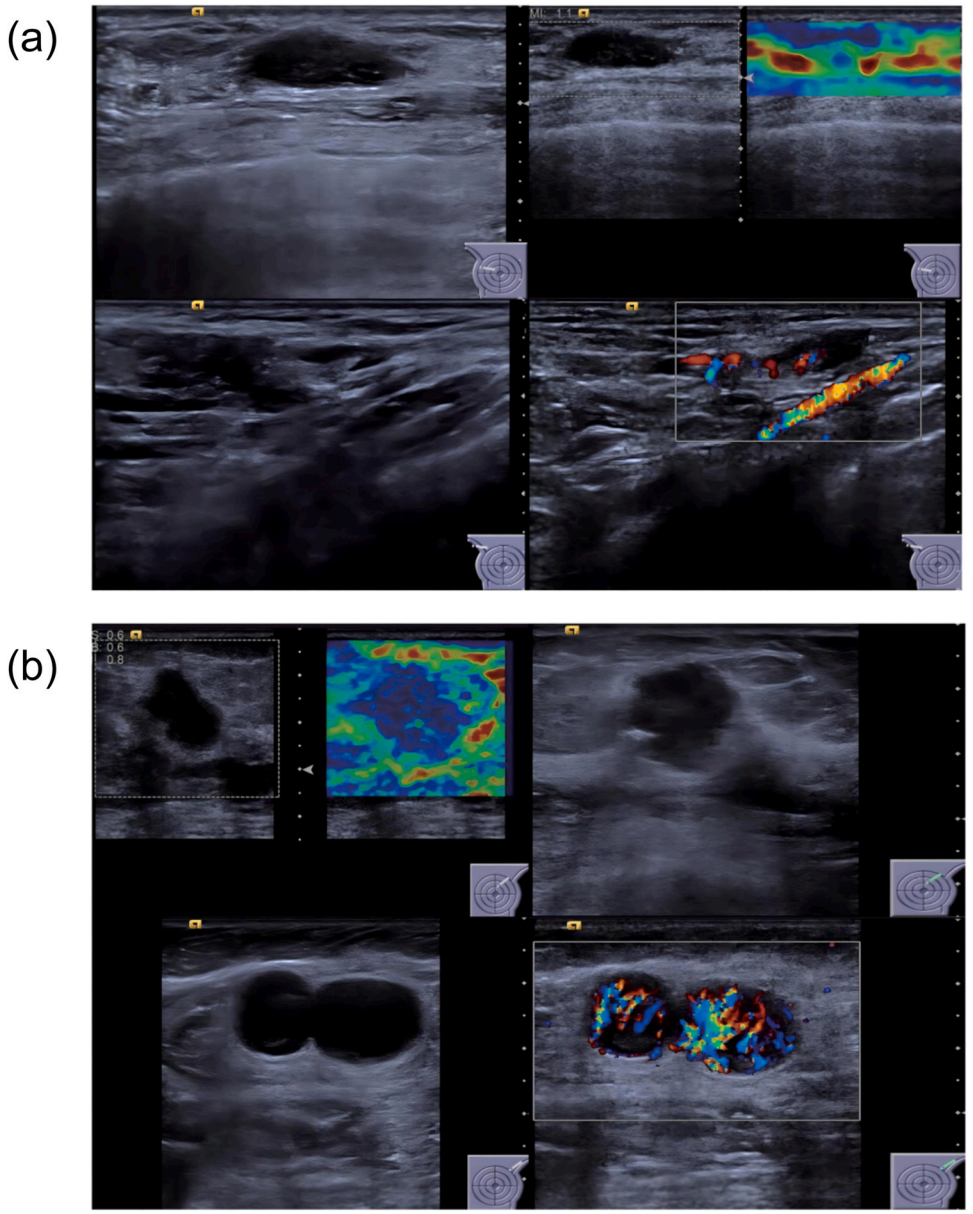

Figure 4. Typical US characteristics in TNBC patients with non-ALNM present or ALNM Present. (**a**) A 47-year-old TNBC patient without ALNM presented with a hypoechoic mass in the right breast, with an elasticity score of 2. The morphology of the left axillary lymph nodes was normal without abnormal blood flow signals. (**b**) A 61-year-old TNBC patient with ALNM presented with an irregular hypoechoic mass in the left breast, surrounded by a hypoechoic halo, with an elasticity score of 5. Abnormal lymph node morphology with abnormal blood flow signal was observed in the left axilla.

validation group, the AUC was 0.929, and in the external validation group, the AUC was 0.891, indicating that the model possesses good predictive capability and exhibits high robustness and generalizability. To improve diagnostic efficiency and accuracy, our study based on a larger sample included imaging characteristics of MG, multimodal US and clinicopathological characteristics. LASSO regression and multivariate logistic regression were used to select the most associated predictors. Moreover, our study incorporated external test to further assess the robustness and generalizability of the model.

According to our study findings, MG_reported_margin, MG_reported_suspicious malignant calcifications, MG_reported_abnormal ALN, elastography score and US_reported_abnormal ALN have been identified as independent predictors for ALNM in TNBC patients.

Tumors with spiculated margins tend to be more malignant, as the tumor cells invade the surrounding tissue and prompt the proliferation of fibrous connective tissue (2). Studies by Xu et al and Cong et al have shown that spiculated margins were an independent predictor for infiltrating BC with ALNM when detected through breast MG

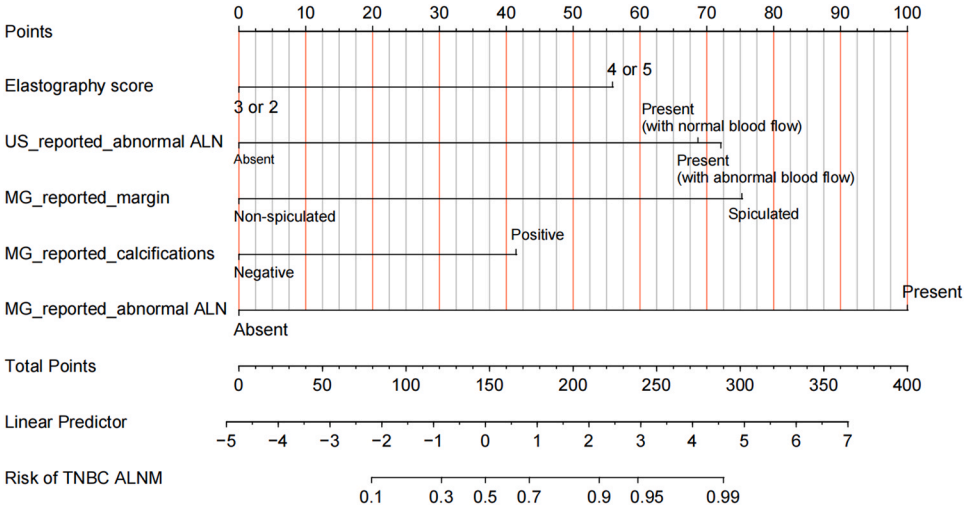

Figure 5. Nomogram prediction model for TNBC ALNM diagnosis.

photography (2,26). However, studies by Song et al and Wang et al on US and MRI characteristics, respectively found no association between margin and ALNM in TNBC patients (15,16). These varying results may be due to differences in sample size, examination methods, and grouping techniques for tumor margins. TNBC tumors typically show fewer calcifications than non-TNBC tumors (4). At Center 1, 48.9% of tumors with suspicious calcifications were in the ALNM group compared to 25.5% in the non-ALNM group, indicating that tumors with suspicious calcifications were more likely to develop ALNM. Multivariate analysis showed that MG_reported_suspicious malignant calcifications were an independent predictor for ALNM in TNBC patients. However, according to Xu et al, who analyzed the characteristics of digital breast tomosynthesis, this was not an independent predictor for ALNM in BC patients (2). They did find that tumors with suspicious calcifications were associated with ALNM in BC patients. US studies reported that the absence of suspicious calcifications in BC tumors showed no statistically significant difference between the metastatic and non-metastatic groups (27). This may be due to the low detection rate of microcalcifications by US, which has lower sensitivity and specificity for microcalcifications compared to MG.

The lymph nodes will lose their normal shape and structure when invaded by a large number of cancer cells. At Center 1, of the 227 patients enrolled, 90 patients had ALNM, with a metastasis rate of 39.6%, similar to previous studies. Studies indicated that the abnormal ALN reported by US, MRI, and breast MG were independent predictors for ALNM prediction in BC patients (2,24,28). Our study demonstrated that MG_reported_abnormal ALN were also an independent predictor for predicting ALNM in TNBC, with sensitivities of 57.8% and specificities of 91.2% for assessing metastatic lymph nodes. Xu et al reported that the sensitivity and specificity of digital breast tomosynthesis imaging in evaluating BC lymph node metastasis were 38.8% and 97.2%, respectively (2). Both our study and Xu et al 's study showed that the sensitivity of MG in evaluating metastatic lymph nodes was limited. This may be due to the limitations of breast MG imaging caused by positioning, where the axillary region of some patients was not fully included in the imaging range, resulting in the incomplete display of ALNM (3). US is the primary method for imaging evaluation of ALNM. Studies have indicated that abnormal ALN reported by US is also an important predictor for ALNM, consistent with our research result (28). Color Doppler US can be used to observe the blood flow distribution in the lymph nodes, helping to differentiate between benign and malignant lymph nodes. Benign lymph nodes present a normal portal blood flow distribution, while malignant lymph nodes often exhibit an absence of portal blood flow or abnormal blood flow distribution. According to Du et al the distribution of lymph node blood flow was a significant predictor of ALNM among BC patients (29). Their study revealed that abnormal blood flow distribution was associated with an increased risk of ALNM, which was consistent with our own research findings.

Ultrasonic elastography is an advanced imaging technique that uses US to measure the elasticity of tissues, which can help differentiate between benign and malignant tumors by analyzing tissue hardness (30). Studies have demonstrated that ultrasound elastography enhances the diagnostic accuracy of ALNM in BC patients and serves as a valuable adjunct for assessing ALN status. Additionally, patients with higher tumor stiffness were more likely to have lymph node positivity (31). Our study revealed that tumor with elasticity score of 4 or 5 was a significant predictor for lymph node metastasis in TNBC patients. Zhao et al analyzed the predictors of ALNM in BC patients and found a significant association between elastography score and ALNM in BC patients (32). However, Zhu et al 's study, which predicted sentinel lymph node metastasis of T_1-T_2 BC based on multimodal US characteristics found no significant difference in elasticity score between

TABLE 4. Diagnostic Performance of the Training Cohort and Test Cohort for Predicting Axillary Lymph Node Metastasis

	AUC (95%CI)	Sensitivity (%)	Specificity (%)	PPV (%)	NPV (%)	Accuracy (%)	Precision (%)	Recall (%)	F1
Training cohort	0.931 (0.890–0.973)	83.3	92.5	88.7	88.7	88.7	88.7	83.3	0.859
Internal test Cohort	0.929 (0.871–0.986)	91.7	77.3	68.8	94.4	82.4	68.8	91.7	0.786
External test cohort	0.891 (0.794–0.987)	83.3	84.8	68.2	92.9	84.4	68.2	83.3	0.750

AUC, area under the receiver operating characteristics curve; PPV, positive predictive value; NPV, negative predictive value; CI, confidence interval.

the negative group and positive group (33). Although elastography scoring is inherently subjective and its association with lymph node metastasis in TNBC patients requires further investigation, its non-invasive nature, ease of application, and high predictive accuracy suggest its considerable potential for clinical implementation.

Our results showed that the quadrant, MG_reported_maximum tumor diameter, MG_reported_skin thickening, US_reported_posterior acoustic decrease, US_reported_hyperechoic halo significantly associated with ALNM in TNBC. However, multivariate logistic regression analysis showed that these predictors were not independent predictors for ALNM in TNBC patients. Notably, the quadrant where the tumor is located remains controversial with regards to lymph node metastasis of TNBC. Our study found a higher positive rate of lymph node metastasis in tumors located in the upper outer quadrant (57.3%) at Center 1, but this was not an independent predictor. Moreover, other studies had reported conflicting opinions on the association between quadrant location and lymph node metastasis in TNBC tumors (5,25). In addition, our results showed a significant positive association between MG_reported_maximum tumor diameter and ALNM in TNBC patients. Furthermore, MG_reported_skin thickening or depression, US_reported_posterior acoustic decrease and US_reported_hyperechoic halo were also associated with lymph node metastasis in TNBC patients, albeit not as independent predictors. Interestingly, a previous study has suggested that these predictors were independent predictors for predicting ALNM in BC (34). These Characteristics showed statistically significant results in univariate analyses, yet were not substantiated as independent predictive factors in the multivariate analyses. The differences in these results could be attributed to the sample size, correlations between variables, or the characteristics of the statistical model employed.

In our study, histological grade, NLR, histological type, Ki-67, and ultrasound features such as mass echogenicity and blood flow, as well as mammographic features including glandular density and mass shape, were not found to be associated with axillary lymph node metastasis (ALNM) in TNBC patients. Higher histological grade and elevated Ki-67 expression are generally indicative of greater tumor malignancy, rapid proliferation, and an increased likelihood of metastasis. Previous studies have demonstrated an association between histological grade, Ki-67, and ALNM in breast cancer (BC) (35,36), which differs from our findings. This discrepancy may be attributed to the lower proportion of Grade I or II tumors and low Ki-67 expression in TNBC compared to other BC subtypes, as well as the limited sample size in our study, which resulted in a scarcity of low-grade and low Ki-67 expression cases, potentially affecting statistical significance. Future studies with larger sample sizes are warranted to validate these findings. Highly invasive tumor cells proliferate at varying rates into surrounding tissues, contributing to the irregular morphology of tumors. Irregular shape has been linked to the biological behavior of tumor metastasis in breast cancer. Although TNBC is a

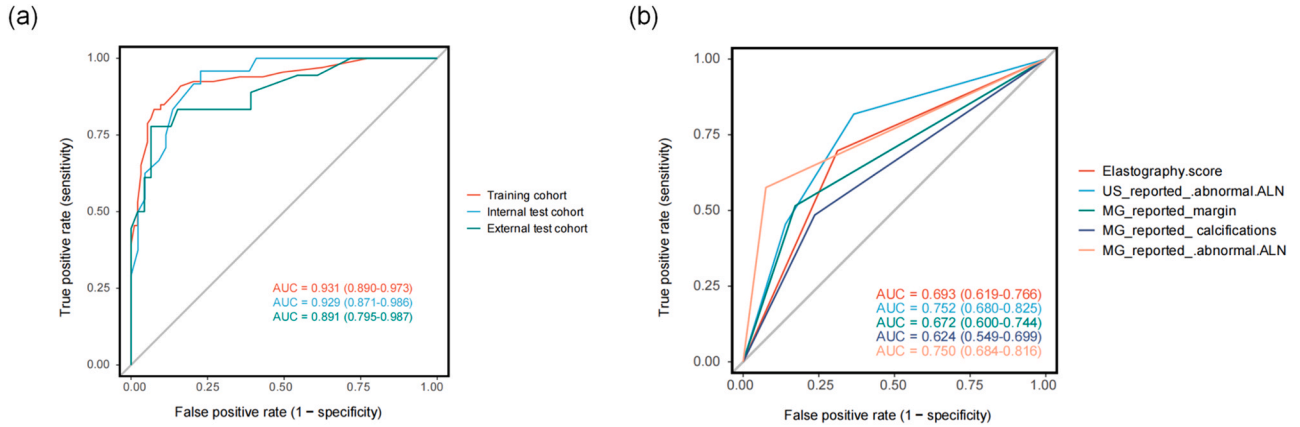

Figure 6. ROC Curves of Characteristics and the nomogram prediction model. (**a**) ROC of 10 Characteristics. (**b**) ROC of the nomogram prediction model in the training cohort and test cohort.

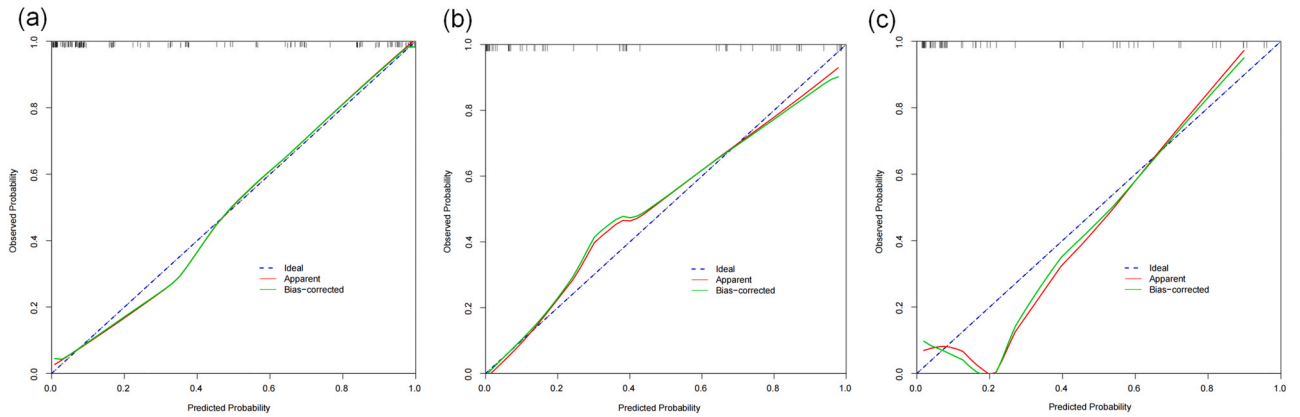

Figure 7. Calibration curve of the nomogram in the training and test cohorts. (**a**) Calibration curves of the nomogram prediction model for the training cohort. (**b**) Calibration curves of the nomogram prediction model for the internal test cohort. **(c)** Calibration curves of the nomogram prediction model for the external test cohort. In this figure, the x-axis represents the predicted risk of ALNM in TNBC patients, while the y-axis represents their actual risk. The gray diagonal line represents the perfect prediction of the model, where the predicted risk equals the actual risk. The black line depicts the predictive performance of the line graph model, with closer proximity to the gray diagonal line indicating better model fitting.

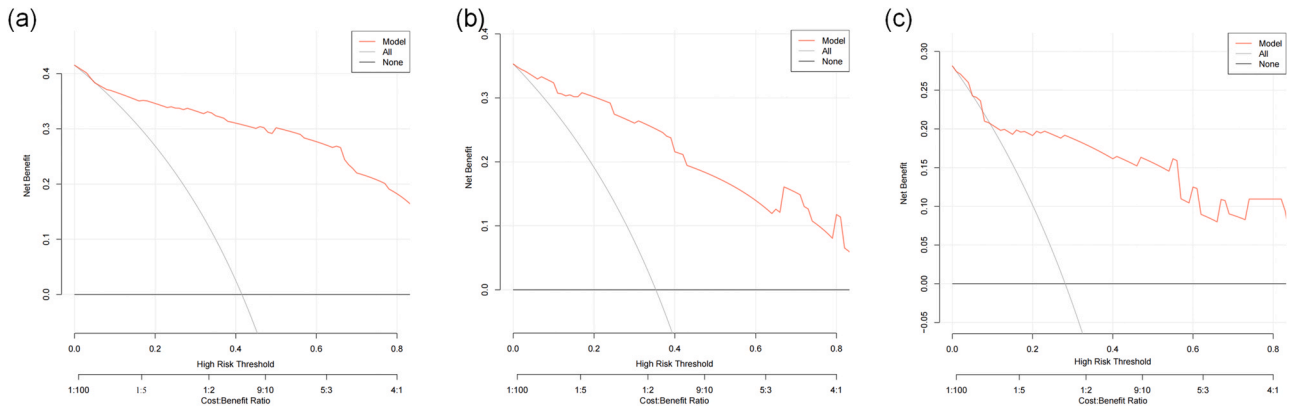

Figure 8. Decision curve analysis of the nomogram in the training and test cohorts. (**a**) Decision curve analysis of the nomogram of the training cohort. (**b**) Decision curve analysis of the nomogram of the internal test cohort. In DCA, the y-axis depicts net benefit, while the x-axis portrays threshold probability. **(c)** Decision curve analysis of the nomogram of the external test cohort. In DCA, the y-axis depicts net benefit, while the x-axis portrays threshold probability. The gray line illustrates the assumption of all patients with ALNM, while the black line depicts the assumption of all patients without ALNM.

highly aggressive tumor, its primary lesions more frequently exhibit regular morphology compared to non-TNBC. In this study, mass shape was not identified as a risk factor for TNBC ALNM, which is consistent with the findings of Song (15) but differs from those of Xu (2). These discrepancies may stem from differences in study populations, and the subjective nature of mass shape evaluation may also have influenced the results. Future studies employing multicenter cohorts and automated imaging analysis techniques are recommended to enhance the reliability of the findings.

Our study provides a limited contribution to the prediction of ALNM in TNBC patients. However, the conflicting opinions on the predictors related to metastasis underscore the need for further investigation. It's important to note that this study has several limitations. Firstly, radiologist-reported characteristics introduce subjectivity, which may impact. In future research, quantitative imaging analysis or deep learning methods could be considered to enhance the consistency and objectivity of feature extraction. Additionally, TNBC is a highly heterogeneous tumor, and a larger sample size would be required to comprehensively analyze the lymph node metastasis predictors of different subtypes of TNBC. Finally, this study only examined mass lesions, and future discussions will also focus on non-mass lesions.

CONCLUSION

In conclusion, MG_reported_margin, MG_reported_suspicious malignant calcifications, MG_reported_abnormal ALN, elastography score and US_report_abnormal ALN had been identified as independent predictors for ALNM in TNBC patients. The predictive model based on these predictors demonstrated significant value for ALNM in TNBC patients.

ETHICS APPROVAL AND CONSENT TO PARTICIPATE

This study complied with the ethical principles of the Declaration of Helsinki (2013 revision) and was approved by the Medical Ethics Committee of the Second Affiliated Hospital of Harbin Medical University (YJSKY2023–298). Written informed consent was obtained from all participants.

FUNDING

This work was supported by the National Natural Science Foundation of China (62172129).

DATA AVAILABILITY

The datasets analyzed during the current study are available from the corresponding author on reasonable request.

DECLARATION OF COMPETING INTEREST

The authors declare that they have no known competing financial interests or personal relationships that could have appeared to influence the work reported in this paper.

ACKNOWLEDGMENTS

This work was supported by the National Natural Science Foundation of China (62172129).

AUTHOR CONTRIBUTIONS

B G and Yt J designed and conceived this study and wrote the manuscript.
Xy L and Yt J performed the statistical analyses.
Y W and Yt J assisted in the implementation of the study and wrote the manuscript.
Xd Z and Y W conducted the external test experiments.
All authors read and approved the final version of the manuscript.

APPENDIX A. SUPPORTING INFORMATION

Supplemental data associated with this article can be found in the online version at doi:10.1016/j.acra.2025.04.031.

REFERENCES

1. Siegel RL, Giaquinto AN, Jemal A. Cancer statistics, 2024. CA Cancer J Clin 2024; 74:12–49. https://doi.org/10.3322/caac.21820
2. Xu M, Yang H, Yang Q, et al. Radiomics nomogram based on digital breast tomosynthesis: preoperative evaluation of axillary lymph node metastasis in breast carcinoma. J Cancer Res Clin Oncol 2023; 149:9317–9328. https://doi.org/10.1007/s00432-023-04859-z
3. Tan H, Wu Y, Bao F, et al. Mammography-based radiomics nomogram: a potential biomarker to predict axillary lymph node metastasis in breast cancer. Br J Radiol 2020; 93:20191019. https://doi.org/10.1259/bjr.20191019
4. Gao B, Zhang H, Zhang SD, et al. Mammographic and clinicopathological features of triple-negative breast cancer. Br J Radiol 2014; 87:20130496. https://doi.org/10.1259/bjr.20130496
5. Chintapally N, Englander K, Gallagher J, et al. Tumor characteristics associated with axillary nodal positivity in triple negative breast cancer. Diseases 2023; 11. https://doi.org/10.3390/diseases11030118
6. Miller KD, Nogueira L, Devasia T, et al. Cancer treatment and survivorship statistics, 2022. CA Cancer J Clin 2022; 72:409–436. https://doi.org/10.3322/caac.21731
7. Giuliano AE, Ballman KV, McCall L, et al. Effect of axillary dissection vs no axillary dissection on 10-year overall survival among women with invasive breast cancer and sentinel node metastasis: the ACOSOG Z0011 (Alliance) randomized clinical trial. JAMA 2017; 318:918–926. https://doi.org/10.1001/jama.2017.11470
8. Giuliano AE, Hunt KK, Ballman KV, et al. Axillary dissection vs no axillary dissection in women with invasive breast cancer and sentinel node metastasis: a randomized clinical trial. JAMA 2011; 305:569–575. https://doi.org/10.1001/jama.2011.90
9. Lyman GH, Giuliano AE, Somerfield MR, et al. American Society of Clinical Oncology guideline recommendations for sentinel lymph node biopsy in early-stage breast cancer. J Clin Oncol 2005; 23:7703–7720. https://doi.org/10.1200/JCO.2005.08.001
10. Saha A, Mukhopadhyay M, Das C, et al. FNAC versus core needle biopsy: a comparative study in evaluation of palpable breast lump. J

Clin Diagn Res 2016; 10. https://doi.org/10.7860/JCDR/2016/15889.7185
11. Agcaoglu O, Aksakal N, Ozcinar B, et al. Factors that affect the false-negative outcomes of fine-needle aspiration biopsy in thyroid nodules. Int J Endocrinol 2013; 2013:126084. https://doi.org/10.1155/2013/126084
12. Jamaris S, Jamaluddin J, Islam T, et al. Is pre-operative axillary ultrasound alone sufficient to determine need for axillary dissection in early breast cancer patients? Medicine (Baltimore) 2021; 100:e25412. https://doi.org/10.1097/MD.0000000000025412
13. Orguc S, Basara I, Pekindil G, et al. Contribution of kinetic characteristics of axillary lymph nodes to the diagnosis in breast magnetic resonance imaging. Balkan Med J 2012; 29:285–289. https://doi.org/10.5152/balkanmedj.2012.010
14. Dent R, Trudeau M, Pritchard KI, et al. Triple-negative breast cancer: clinical features and patterns of recurrence. Clin Cancer Res 2007; 13:4429–4434. https://doi.org/10.1158/1078-0432.CCR-06-3045
15. Song SE, Woo OH, Cho Y, et al. Prediction of axillary lymph node metastasis in early-stage triple-negative breast cancer using multiparametric and radiomic features of breast MRI. Acad Radiol 2023; 30(2):S25–S37. https://doi.org/10.1016/j.acra.2023.05.025
16. Wang J, Lu X, Zheng X, et al. Clinical value of preoperative ultrasound signs in evaluating axillary lymph node status in triple-negative breast cancer. J Oncol 2022; 2022:2590647. https://doi.org/10.1155/2022/2590647
17. Chang JM, Leung J, Moy L, et al. Axillary nodal evaluation in breast cancer: state of the art. Radiology 2020; 295:500–515. https://doi.org/10.1148/radiol.2020192534
18. Adler DD, Carson PL, Rubin JM, et al. Doppler ultrasound color flow imaging in the study of breast cancer: preliminary findings. Ultrasound Med Biol 1990; 16:553–559. https://doi.org/10.1016/0301-5629(90)90020-d
19. Maxwell F, de Margerie MC, Bricout M, et al. Diagnostic strategy for the assessment of axillary lymph node status in breast cancer. Diagn Interv Imaging 2015; 96:1089–1101. https://doi.org/10.1016/j.diii.2015.07.007
20. Itoh A, Ueno E, Tohno E, et al. Breast disease: clinical application of US elastography for diagnosis. Radiology 2006; 239:341–350. https://doi.org/10.1148/radiol.2391041676
21. Fan M, He T, Zhang P, et al. Heterogeneity of diffusion-weighted imaging in tumours and the surrounding stroma for prediction of Ki-67 proliferation status in breast cancer. Sci Rep 2017; 7:2875. https://doi.org/10.1038/s41598-017-03122-z
22. Zhu S, Wu Y, Song B, et al. Recent advances in targeted strategies for triple-negative breast cancer. J Hematol Oncol 2023; 16:100. https://doi.org/10.1186/s13045-023-01497-3
23. Yu F, Hang J, Deng J, et al. Radiomics features on ultrasound imaging for the prediction of disease-free survival in triple negative breast cancer: a multi-institutional study. Br J Radiol 2021; 94:20210188. https://doi.org/10.1259/bjr.20210188
24. Song D, Yang F, Zhang Y, et al. Dynamic contrast-enhanced MRI radiomics nomogram for predicting axillary lymph node metastasis in breast cancer. Cancer Imaging 2022; 22:17. https://doi.org/10.1186/s40644-022-00450-w
25. Fong W, Tan L, Tan C, et al. Predicting the risk of axillary lymph node metastasis in early breast cancer patients based on ultrasonographic-clinicopathologic features and the use of nomograms: a prospective single-center observational study. Eur Radiol 2022; 32. https://doi.org/10.1007/s00330-022-08855-8
26. Cong Y, Wang S, Zou H, et al. Imaging predictors for nonsentinel lymph node metastases in breast cancer patients. Breast Care (Basel) 2020; 15:372–379. https://doi.org/10.1159/000501955
27. Guo Q, Dong Z, Zhang L, et al. Ultrasound features of breast cancer for predicting axillary lymph node metastasis. J Ultrasound Med 2018; 37:1353–1354. https://doi.org/10.1002/jum.14469
28. Chen J, Li CX, Shao SH, et al. The association between conventional ultrasound and contrast-enhanced ultrasound appearances and pathological features in small breast cancer. Clin Hemorheol Microcirc 2022; 80:413–422. https://doi.org/10.3233/CH-211291
29. Du LW, Liu HL, Gong HY, et al. Adding contrast-enhanced ultrasound markers to conventional axillary ultrasound improves specificity for predicting axillary lymph node metastasis in patients with breast cancer. Br J Radiol 2021; 94:20200874. https://doi.org/10.1259/bjr.20200874
30. Athanasiou A, Tardivon A, Tanter M, et al. Breast lesions: quantitative elastography with supersonic shear imaging–preliminary results. Radiology 2010; 256:297–303. https://doi.org/10.1148/radiol.10090385
31. Pu H, Zhao LX, Yao MH, et al. Conventional US combined with acoustic radiation force impulse (ARFI) elastography for prediction of triple-negative breast cancer and the risk of lymphatic metastasis. Clin Hemorheol Microcirc 2017; 65:335–347. https://doi.org/10.3233/CH-16196
32. Zhao Q, Sun JW, Zhou H, et al. Pre-operative conventional ultrasound and sonoelastography evaluation for predicting axillary lymph node metastasis in patients with malignant breast lesions. Ultrasound Med Biol 2018; 44:2587–2595. https://doi.org/10.1016/j.ultrasmedbio.2018.07.017
33. Zhu Y, Lv W, Wu H, et al. A preoperative nomogram for predicting the risk of sentinel lymph node metastasis in patients with T1-2N0 breast cancer. Jpn J Radiol 2022; 40:595–606. https://doi.org/10.1007/s11604-021-01236-z
34. Bai X, Wang Y, Song R, et al. Ultrasound and clinicopathological characteristics of breast cancer for predicting axillary lymph node metastasis. Clin Hemorheol Microcirc 2023; 85:147–162. https://doi.org/10.3233/CH-231777
35. Gao X, Luo W, He L, et al. Nomogram models for stratified prediction of axillary lymph node metastasis in breast cancer patients (cN0). Front Endocrinol (Lausanne) 2022; 13:967062. https://doi.org/10.3389/fendo.2022.967062
36. Fu Y, Jiang J, Chen S, et al. Establishment of risk prediction nomogram for ipsilateral axillary lymph node metastasis in T1 breast cancer. Zhejiang Da Xue Xue Bao Yi Xue Ban 2021; 50:81–89. https://doi.org/10.3724/zdxbyxb-2021-0013